

Tailor-Made Poly(methyl acrylate) bearing Amantadine Functionality (Amino Adamantyl) via Atom Transfer Radical Polymerization (ATRP). A Precursor of a Supramolecular Cross-Linked Polymer

A. Amalin Kavitha and Nikhil K. Singha*

Rubber Technology Centre, Indian Institute of Technology, Kharagpur, India 721302

Received February 3, 2009; Revised Manuscript Received May 27, 2009

ABSTRACT: Poly(methyl acrylate)s bearing an amino adamantyl group were prepared via atom transfer radical polymerization (ATRP). The amino adamantyl (amantadine) group was incorporated into the polymer by homopolymerization as well as by copolymerization of acrylate bearing amantadine functional group. The rate of ATRP was slow compared to the rate of ATRP of methyl acrylate or adamantyl containing acrylate. It is due to the interaction of amine group of amantadine with Cu catalyst. ¹H NMR, matrix assisted laser desorption ionization time-of-flight mass spectrometry (MALDI–TOF–MS) and gel permeation chromatography (GPC) analysis showed that the polymers had well-defined molecular weight and amino adamantyl functional group. Interestingly, this amine group was further reacted with epoxy group of the tailor-made poly(glycidyl methacrylate) (PGMA) to produce hydrogen-bonded polymers having porous network structure. It was evidenced by field-emission scanning electron microscopy (FESEM) analysis, differential scanning calorimetry (DSC) analysis as well as by molecular modeling.

Introduction

Since its discovery in 1995, atom transfer radical polymerization (ATRP) has rapidly attracted growing interest of polymer chemists, because of its versatility in the synthesis of polymers with predictable molecular weights, low polydispersities, and specific functionalities.^{1,2} In ATRP, monomers as well as initiators containing functional groups are most often used in order to synthesize functional polymers.^{1–4} Anto et al.⁵ reported that the functional groups interfere with the ATRP catalytic system. It is therefore often necessary to use the functional groups in a protected form.^{5–7} Chaumont et al.⁸ reported the end functionalization of bromo-terminated polystyrene with tetraphenylethane-based derivatives by living free radical polymerization. Matyjaszewski et al.⁶ reported carboxylic acid terminated polystyrene by ATRP. This kind of end functionalized polymers can be used to prepare polymer with well-defined architectures, such as various block copolymers, as well as grafted and hyperbranched materials. The acrylic-based polymers have interesting optical and mechanical properties. They are bioinert or biocompatible, and are therefore finding important applications in industrial uses as well as in the biomedical field.⁹ The amine functional group is one of the most fundamental motifs found in chemistry and biology, and it has been studied extensively in the past century.¹⁰ Amino and carboxylate substituted adamantane derivatives have proven to be valuable tools in both physical organic and medicinal chemistry.¹¹ Amine groups are also used to react with epoxy-containing polymers.

This investigation reports the incorporation of amino adamantyl (amantadine) functional groups into the poly(methyl acrylate)s by using ATRP. Structurally, amantadine (C₁₀H₁₅NH₂) is an amino derivative of the parent molecule adamantane (C₁₀H₁₆), a cage-like hydrocarbon that has pharmaceutical significance.¹² It is commonly available under the trade names of Symadine and Symmetrel. It is mainly used as antiviral¹³ and anti-Parkinsonian¹⁴ drugs and has been established very effective in the

prophylaxis and treatment of influenza A virus infections.^{15–19} Polymers containing specialty functional groups can be used for the treatment of various diseases.^{20,21} Adamantane, the parent molecule of amantadine is highly thermally stable.²² Radical polymerization using adamantyl containing monomer or initiator leads to faster polymerization rate.^{22,23} Polymers containing adamantyl group have high thermal stability as well as higher glass transition temperature (*T_g*). The incorporation of the amantadine into the polymers as well as the post polymerization reaction of this active amine group can lead to several potential applications such as high temperature resistant material and materials for biomedical applications.

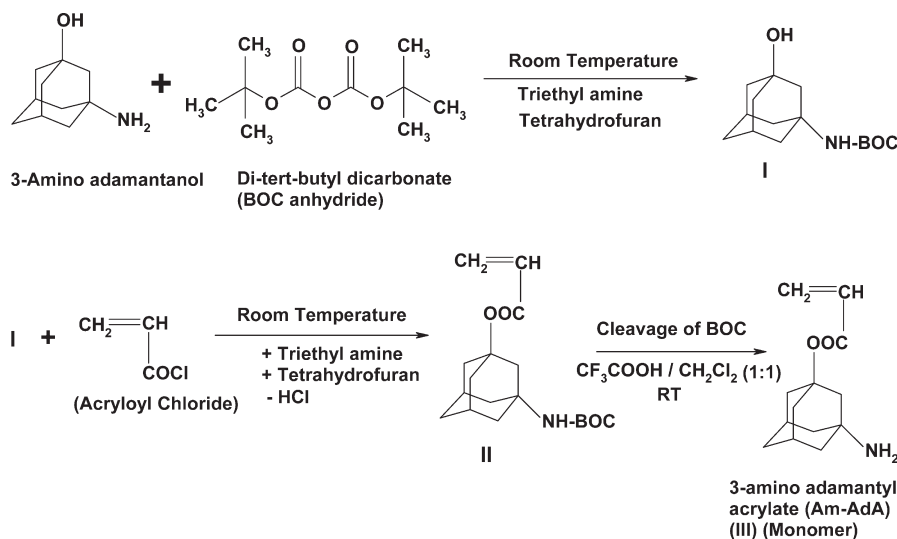
The present study reports the synthesis of methyl acrylate (MA) bearing amantadine via protection–deprotection synthon and the first example of ATRP of this specialty monomer. The polymers were characterized by ¹H NMR, MALDI–TOF, and GPC analysis. Interestingly, the active –NH₂ group was reacted with the epoxy group in the polyglycidyl methacrylate (PGMA) leading to a hydrogen-bonded porous network, as evidenced by SEM, FT-IR, and DSC analysis.

Experimental Section

Materials. 3-Amino-1-adamantanol (96%), 2-bromoisobutyl bromide (98%), di-*tert*-butyl dicarbonate (99%), 1-adamantane methanol (99%, Aldrich) and trifluoroacetic acid (TFA) (99%, Aldrich) were purchased from Aldrich Chemicals USA, and were used as received. The monomers, glycidyl methacrylate (GMA) (97%, Aldrich), methyl methacrylate (MMA) (99%, Aldrich) and methyl acrylate (MA) (99%, Aldrich) were purified by vacuum distillation prior to use. Acryloyl chloride (96%, Fluka) was distilled and the fraction boiling between 74 and 79 °C was collected and stored in refrigerator prior to use. AdMA was synthesized from 1-adamantane methanol and acryloyl chloride following standard procedures.²⁴ Triethylamine (TEA, SD. Fine chemicals, Mumbai, India) was dried over KOH and distilled before use. Dichloromethane (DCM, SD. Fine chemicals, Mumbai, India), was dried over anhydrous CaCl₂ and was distilled over anhydrous P₂O₅ before use. Tetrahydrofuran

*Corresponding author. Telephone: +91 3222 283178. Fax.: +91 3222 255303. E-mail: nks@rtc.iitkgp.ernet.in.

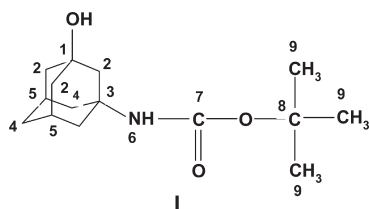
Scheme 1. Synthesis of 3-Amino Adamantyl Acrylate (Am-AdA) (III) (Monomer)



(THF, SD. Fine chemicals, Mumbai, India) was refluxed over sodium and distilled twice before use. Toluene (SD. Fine chemicals, Mumbai, India) was purified by vacuum distillation over CaH_2 . Azobisisobutyronitrile (AIBN, ACROS Chemical, 98%) was recrystallized from methanol. CuBr (Aldrich, USA) was purified by washing with glacial acetic acid, followed by diethyl ether, and then dried under vacuum. Methyl 2-bromopropionate (MBrP) (97%), ethyl 2-bromoisobutyrate (EBiB) (98%), 4,4'-di(5-nonyl)-2,2'-bipyridine (dNbpy) (97%), and N,N,N',N'',N'' -pentamethyl diethylenetriamine (PMDETA) were obtained from Aldrich USA and were used as received.

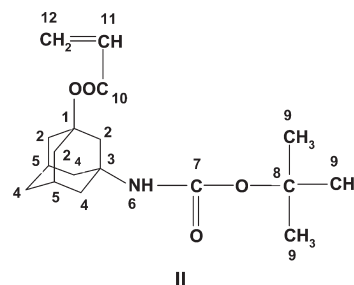
Synthesis. The monomer bearing amino adamantyl group was synthesized according to Scheme 1.

Synthesis of Monomer, 3-Amino Adamantyl Acrylate (Am-AdA) (III). *Synthesis of Compound I.* A solution of di-tert-butyl dicarbonate (3.64 g, 1.67×10^{-2} mol) in 10 mL of dry THF was slowly added into a stirred solution of 3-amino adamantanol (4.00 g, 2.39×10^{-2} mol) in 10 mL of dry THF was taken in a 100 mL three-necked round-bottom flask under cooled in a ice bath condition. Triethyl amine (TEA) (1.20 g, 1.19×10^{-2} mol) was added into the round-bottomed flask under nitrogen atmosphere. And the stirring was continued for 5 h. Then the reaction mixture was stirred at room temperature for 12 h. After the removal of THF, 20 mL of ethyl acetate was added to the reaction mixture. The organic layer was washed with distilled water, later with brine solution and was finally dried over anhydrous Na_2SO_4 . The organic layer was filtered and concentrated. The final product was recrystallized from methanol and the resultant product was pale yellowish solid. Yield = 4.52 g (80%). ^1H NMR, δ = 1.37 (s, 9H, C_9 , CH_3), 1.55 (s, 6H, $\text{C}(2)\text{H}_2$), 1.61–1.76 (m, 6H, $\text{C}(4)\text{H}_2$), 2.13 (s, 2H, $\text{C}(5) - \text{CH}-$), 4.72 ($-\text{OH}$) and 5.76 ($-\text{NH}-\text{CO}-$) ppm; ^{13}C NMR, δ = 70.21 (C_1 , $\geq \text{C}-\text{OH}$), 35.78 (C_2), 67.9 (C_3 , $\geq \text{C}-\text{NH}-$), 40.25 (C_4), 31.53 (C_5), 175.01 (C_7 , $-\text{NHCO}-$), 80.65 (C_8 , $-\text{OC}\leq$), and 33.25 (C_9) ppm.



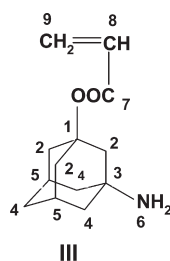
Synthesis of Compound II. Compound I (4.00 g, 1.49×10^{-2} mol) was dissolved in 10 mL of dry THF and dry triethyl

amine (1.20 g, 1.18×10^{-2} mol) were taken up in a 100 mL three-necked round-bottom flask. The contents were cooled with ice, and acryloyl chloride (2.72 g, 3.02×10^{-2} mol) was added dropwise under nitrogen atmosphere for 5 h. The reaction mixture was brought to room temperature and was left stirring for another 12 h. The reaction mixture was then poured into water and extracted with dichloromethane. The organic layer was washed with water and brine solution and was finally dried over anhydrous Na_2SO_4 . The organic layer was filtered and the pure product was obtained as a viscous liquid via vacuum distillation. Yield = 4.97 g (75%). ^1H NMR, δ = 1.37 (s, 9H, C_9 , CH_3), 1.54 (s, 6H, $\text{C}(2)\text{H}_2$), 1.60–1.76 (m, 6H, $\text{C}(4)\text{H}_2$), 2.10 (s, 2H, $\text{C}(5) - \text{CH}-$), 5.76 ($-\text{NH}-\text{CO}-$), 5.19 and 5.70 (s, 3H, $\text{CH}_2=\text{CH}-$ (C_{12} and C_{11}), ppm; ^{13}C NMR, δ = 81.37 (C_1), 35.77 (C_2), 67.6 (C_3 , $\geq \text{C}-\text{NH}-$), 40.23 (C_4), 31.53 (C_5), 175.11 (C_7 , $-\text{NHCO}-$), 80.66 (C_8 , $-\text{OC}\leq$), 33.23 ($\text{C}_9 - \text{CH}_3$), 170.02 (C_{10} , $\text{C}=\text{O}$), 130.46 (C_{11} , $-\text{CH}=\text{CH}_2$) and 128.01 (C_{12} , $\text{CH}_2=$) ppm.



Synthesis of Compound III. Compound II (4.50 g, 1.40×10^{-2} mol) was dissolved in 3 mL of dry dichloromethane, and the resulting solution was placed in a three-neck round-bottom flask. A mixture of trifluoroacetic acid and dry dichloromethane mixture (TFA: DCM) at 1:1 equivalence was added slowly to the round-bottom flask under stirring at room temperature. The final products were poured into distilled water and were extracted with dichloromethane. The extract was washed with water, brine solution and dried over anhydrous sodium sulfate, the organic layer was filtered and passed through the column and concentrated. The final product was yellowish viscous liquid yielding at 3.23 g (72%). ^1H NMR, δ = 1.56 (s, 6H, $\text{C}(2)\text{H}_2$), 1.61–1.76 (m, 6H, $\text{C}(4)\text{H}_2$), 2.12 (s, 2H, $\text{C}(5) - \text{CH}-$), 3.74 ($-\text{NH}_2$, C_6), 5.20 and 5.71 (3H, $\text{CH}_2=\text{CH}-$, (C_9 and C_8)) ppm; ^{13}C NMR, δ = 81.32 (C_1),

35.75 (C_2), 66.8 (C_3 , $\geq C-NH_2$), 40.23 (C_4), 31.53 (C_5), 170 (C_7 , $C=O$), 130.44 (C_8 , $-CH=CH_2$) and 128.01 (C_9 , $CH_2=CH-$) ppm.



Atom Transfer Radical Polymerization (ATRP). *Homopolymerization of 3-Amino Adamantyl Acrylate (Am-AdA) (III).* In a typical polymerization procedure, CuBr (0.025 g, 1.80×10^{-4} mol) and the ligand, dNbpy (0.073 g, 1.80×10^{-4} mol) were placed in a 50 mL three neck round-bottom flask. The monomer, Am-AdA (III) (2.00 g, 9.04×10^{-3} mol) was then added. The flask was equipped with a condenser in one neck and a silicone rubber septum in the other. The polymerization was carried out under nitrogen atmosphere. The polymerization was started by adding methyl 2-bromo propionate (0.030 g, 1.80×10^{-4} mol) and was carried out at 70 °C. At different time intervals, the sample was withdrawn under nitrogen atmosphere and a part of it was used for the gravimetric determination for monomer conversion. The remaining sample was passed through an alumina column to remove the catalyst and then was dried under vacuum at 45 °C. Yield: 0.99 g (50%). $M_{n(GPC)} = 5572$ ($M_{n(theo)} = 5611$) and $M_w/M_n = 1.33$. 1H NMR, $\delta = 1.38$ and 2.28 ($>CH_2$ and $>CH-$ of main chain backbone), 1.57 (s, 6H, $>CH_2$ (b₁)), 1.63–1.79 (m, 6H, $>CH_2$ (b₃)), 2.01 (s, 2H, $>CH-$ (b₂)), 3.74 ($-NH_2$) and 3.65 ($>CH-Br$, chain end group of the polymer) ppm.

Copolymerization of Am-AdA (III) and Methyl Acrylate (MA). In this case, the copolymerization of Am-AdA and MA was carried out at a feed ratio of 40:60 respectively. In a typical polymerization procedure, CuBr (0.032 g, 2.26×10^{-4} mol) and dNbpy (0.092 g, 2.26×10^{-4} mol), were taken in a three neck round-bottom flask. The monomers, Am-AdA (III) (2.00 g, 9.04×10^{-3} mol) and MA (1.16 g, 1.35×10^{-2} mol) were added into the flask under nitrogen atmosphere. The flask was equipped with a condenser in one neck and a silicone rubber septum in the other. Then the flask was placed into the oil bath already heated at 70 °C. The copolymerization was started by adding methyl 2-bromo propionate (0.037 g, 2.26×10^{-4} mol) into the flask. At different time intervals, the sample was taken out under nitrogen atmosphere. The copolymer conversion was calculated gravimetrically. The copolymer was purified by passing through an alumina column to remove the catalyst and then was dried under vacuum at 45 °C. Yield: 1.42 g (45%). $M_{n(GPC)} = 6300$ ($M_{n(theo)} = 6425$) and $M_w/M_n = 1.38$. 1H NMR, $\delta = 1.37$ and 2.29 ($>CH_2$ and $>CH-$ of main chain backbone), 1.57 (s, 6H, $>CH_2$ of adamantyl protons (b₁)), 1.63–1.79 (m, 6H, $>CH_2$ of adamantyl protons (b₃)), 2.01 (s, 2H, $>CH-$ of adamantyl protons (b₂)), 3.55 (3H, $-OCH_3$ of MA protons), 3.74 ($-NH_2$) ppm. The copolymer composition determined by 1H NMR was 25% of PAm-AdA and 75% of PMA.

Synthesis of the Diblock Copolymer (PAm-AdA-b-PMMA). The diblock copolymer was synthesized by the chain extension experiment of PAm-AdA using as a macroinitiator (0.50 g, 8.97×10^{-5} mol, $M_{n(GPC)} = 5572$, $M_w/M_n = 1.33$) by the addition of fresh MMA (0.89 g, 8.97×10^{-3} mol) as the monomer. Synthesis of the diblock copolymer was carried out on the similar method as described for the homopolymerization of Am-AdA. The different chemicals were used, CuBr (0.012 g, 8.97×10^{-5} mol) as catalyst, PMDETA (0.015 g, 8.97×10^{-5} mol) as ligand, and PAm-AdA (0.50 g, 8.97×10^{-5} mol) as macroinitiator instead of methyl

2-bromopropionate. Yield: 0.79 g (57%). $M_{n(GPC)} = 8817$ ($M_{n(theo)} = 8876$) and $M_w/M_n = 1.35$. 1H NMR, $\delta = 0.81$ –1.04 (3H, $-CH_3$ of PMMA), 1.20–2.10 (2H, $>CH_2$ protons of PMMA unit and 14H of $>CH_2$, $>CH-$ of the PAm-AdA (adamantyl group) initiator part), 3.50 (3H, $-OCH_3$ of PMMA), 3.74 (2H, $-NH_2$ of PAm-AdA initiator part) ppm.

Preparation of Polyglycidyl Methacrylate (PGMA). PGMA was prepared by using GMA:CuBr:PMDETA:EBiB at the ratio of 50:1:1:1 at room temperature via ATRP method. The same procedure was adopted as for the ATRP of Am-AdA (III) as described earlier. Yield: 1.81 g (91%). $M_{n(GPC)} = 5865$ ($M_{n(theo)} = 5911$) and $M_w/M_n = 1.21$. 1H NMR, $\delta = 0.92$ to 2.16 (5H, $-CH_3$ and $>CH_2$ of main chain backbone), 2.62 and 2.83 (2H, $>CH_2$ of epoxy group), 3.23 (1H, $>CH-$ of epoxy group), 3.79 and 4.30 (2H, $-OCH_2$) ppm.

One-Pot Synthesis of Hydrogen-Bonded Polymer (VI). Poly (glycidyl methacrylate) (PGMA) (1.00 g, 1.70×10^{-4} mol) ($M_n = 5865$, $M_w/M_n = 1.21$) and PAm-AdA (VI) (0.95 g, 1.70×10^{-4} mol) ($M_n = 5572$ and $M_w/M_n = 1.33$) were dissolved in 25 mL of dry toluene in a 100 mL round-bottom flask under nitrogen atmosphere. The mixture was refluxed at 120 °C for 9 h under constant stirring. Then the reaction mixture was allowed to cool at room temperature. The pale yellowish white colored solid material was precipitated itself during the reaction. The resultant material was dried under vacuum for 24 h. Yield: 1.44 g (74%).

Instrumentation. The GPC measurement was performed at ambient temperature using a Viscotek GPC equipped with a refractive index detector (model VE 3580). The polymer solution was passed through two Viscogel GPC columns (model GMHHR-M #17392) connected in series. The GPC columns were mixed bed columns having pore size of 30–650 Å and were suitable for the polymer of medium to high molecular weights (exclusion limit $M_n = 1 \times 10^6$). THF was used as eluent at room temperature with a flow rate of 1.0 mL/min. Linear PMMA standards (Polymer Laboratories) were used as calibration standard. Data acquisition and processing were performed using Viscotek OMNI-01 software. 1H (400 MHz) and ^{13}C (125 MHz) NMR spectra were recorded on a Bruker 400 spectrometer using $CDCl_3$ as solvent which had a small amount of TMS as internal standard. Infrared spectra were recorded on a Perkin-Elmer, Inc. version 5.0.1 spectrophotometer. In this case a dilute solution of the polymer sample in chloroform was film cast over KBr cells and then the IR spectra were recorded. FTIR spectra were recorded in the range of 4000–400 cm^{-1} . Mass spectra were acquired on a Perceptiv Biosystems Voyager Elite MALDI-TOF mass spectrometer, equipped with a nitrogen laser (wavelength 337 nm). Polymer samples, 2,5-dihydroxybenzoic acid (used as matrix) and sodium trifluoroacetate (used as a cationic agent) were dissolved in THF (10 mg/mL solutions of each component) and the resulting solutions were mixed at 100/100/1 volume ratio. All the spectra were averaged over 128 laser shots. Differential Scanning Calorimetry (DSC) analysis was carried out using a Pyris Diamond DSC, Perkin Elmer (U.K.), under nitrogen atmosphere at a heating rate of 20 °C/min. The glass transition temperature (T_g) was calculated from the inflection point in the second heating cycle. The baseline was calibrated by scanning the temperature domain of the experiments with an empty pan. The enthalpy was calibrated with an indium standard, as well as the heat capacity was calibrated by measuring with sapphire disk supplied by Perkin-Elmer Instruments. The temperature calibration was performed with different metal standards at the various heating rates. UV-vis spectroscopic measurements were performed at 25 °C on a Hewlett-Packard diode array UV-vis spectrometer, using a quartz UV cell. UV and visible electronic spectra were recorded at a concentration of 5.0×10^{-4} mol/L in tetrahydrofuran in $\lambda = 190$ –1000 nm. The morphological study of the polymers was performed using an SEM model JSM800 manufactured by JEOL at 20 kV acceleration voltage at room temperature. The pore size of the polymer was measured using

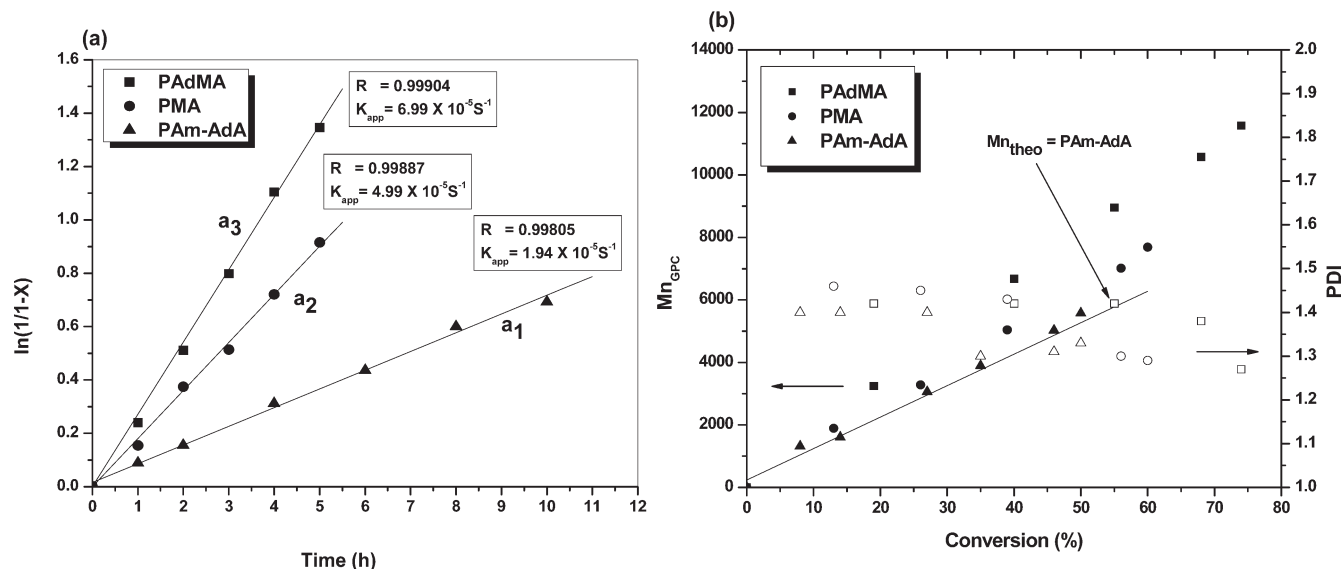


Figure 1. (a) Kinetic plots of $\ln(1/[1-x])$ versus reaction time t , and (b) the dependence of the number-average molecular weights (M_n) and molecular weight distributions ($PDI = M_w/M_n$) on the monomer conversion for the atom transfer radical polymerization in bulk at 90 °C [$M_0/CuBr/dNbpy/MBrP$, 50:1:1:1]. (▲) Poly (amino adamantyl acrylate) (PAm-AdA), (●) Poly (methyl acrylate) (PMA) and (■) Poly (adamantyl methyl acrylate) (PAdMA).

Scheme 2. Atom Transfer Radical Polymerization for Incorporating the Amino Adamantyl Group in the Polymer: (a) Homo Polymerization of Amino Adamantyl Acrylate (Am-AdA) (III); (b) Copolymerization of Amino Adamantyl Acrylate (Am-AdA) (III) and Methyl Acrylate (MA)

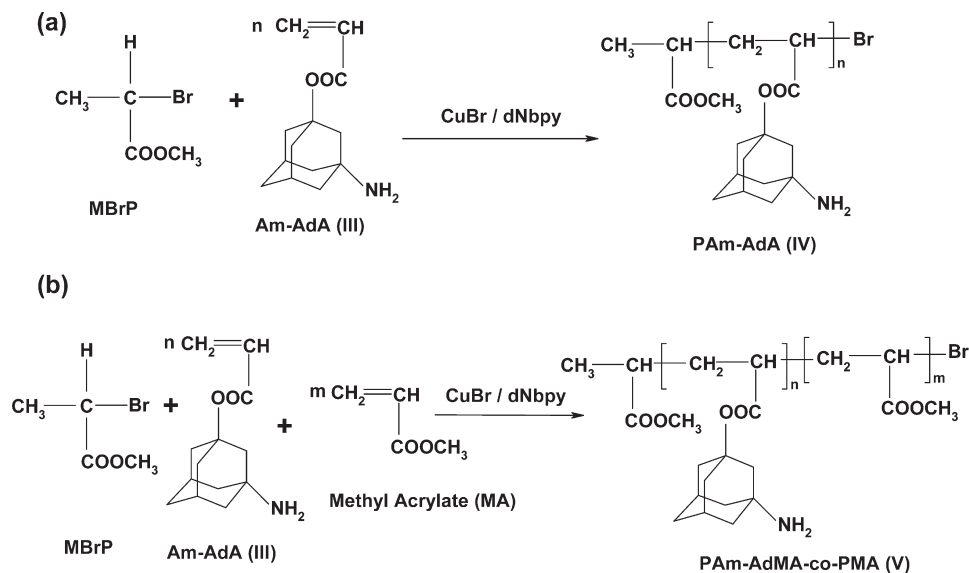


image processing software, “Image tool version 3.0”. The modeling study for hydrogen-bonded polymer was performed with the DMol³ molecular modeling software. The optimization of the hydrogen-bonded structure was made using Gaussian 03 Package.

Results and Discussion

The synthesis of 3-amino adamantyl acrylate (III), an amino adamantyl (amantadine) containing monomer was carried out by a three-step synthetic procedure (Scheme 1). In this case the first step is the reaction between 3-amino adamantanol and di-*tert*-butyl dicarbonate to generate amine protected 3-amino adamantanol (I). In the second step this amine protected compound was reacted with acryloyl chloride to obtain structure II (in Scheme 1), the amine-protected monomer. The final step is the cleavage of di-*tert*-butyl dicarbonate by the addition of 1:1 mixture of trifluoroacetic acid/dichloromethane to obtain the resultant monomer,

3-amino adamantyl acrylate (III) (Am-AdA). The Am-AdA was polymerized using CuBr/dNbpy as catalyst and methyl bromo propionate as initiator (Scheme 2). The plot of $\ln(1/[1-x])$ vs reaction time shows linear indicating the concentration of active species is constant throughout the reaction. The comparative kinetic plots of the ATRP of Am-AdA, MA and AdMA (adamantyl methyl acrylate) are shown in Figure 1a. The rate of polymerization of Am-AdA is slower than that of MA and AdMA. Figure 1b shows that there is gradual increase in molecular weight (M_n) with conversion maintaining relatively low polydispersity index ($PDI = M_w/M_n$). The conversions as well as the molecular weights of the polymers at different time interval are much less in the ATRP of Am-AdA than that in the ATRP of AdMA (Figure 1, parts a and b). The polydispersity index of the PAm-AdA is relatively broader than PAdMA or PMA. It is due to the probable coordination between copper catalyst and amine group in the monomer which slows the

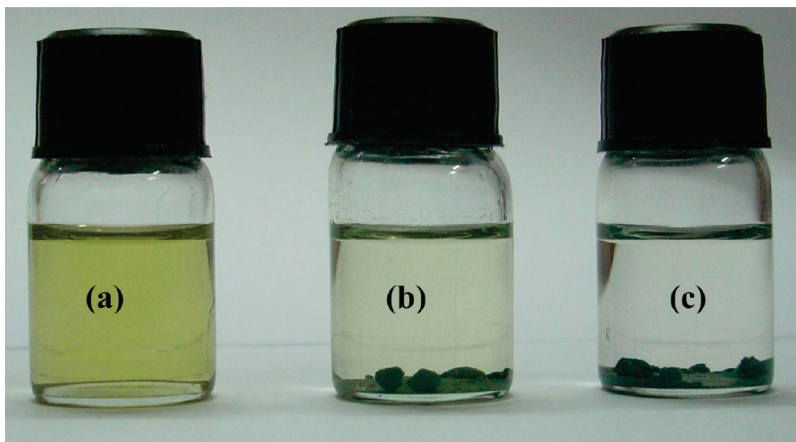


Figure 2. Solutions of CuBr in amino adamantyl acrylate (Am-AdA) (4 mg/1 mL) (a), CuBr in adamantyl methyl acrylate (AdMA) (4 mg/1 mL) (b), and CuBr in methyl acrylate (MA) (4 mg/1 mL) (c).

dynamics of the equilibrium between the dormant species and active species. Controlled experiments were carried out to elucidate the nature of interaction between copper catalyst and $-\text{NH}_2$. Figure 2 indicates that the solution of CuBr and Am-AdA is homogeneous (Figure 2a) whereas the solution of CuBr in AdMA or in MA is heterogeneous (Figure 2, parts b and c).

Figure 3 shows the UV-vis spectra of the Am-AdA and the mixture of Am-AdA and CuBr in THF. The solution of Am-AdA in THF shows a characteristic absorption peak at 334 nm while Am-AdA/CuBr shows at 310 nm wavelength (Figure 3a). After the addition of CuBr into Am-AdA solution, the color gradually changed from light yellow to green at room temperature, and the intensity of the characteristic absorption peak decreased over 10 h (Figure 3b). The decrease in the intensity of the absorption peak at 310 nm is due to the interaction between NH_2 moieties and Cu ions. It is reported that aliphatic amines can interact with copper ions.^{25–28} Figure 2 shows that CuBr is soluble in Am-AdA, but insoluble in AdMA or MA. It indicates that $-\text{NH}_2$ group in Am-AdA form complex with CuBr. Haddleton et al.²⁸ reported that the reactivity of aminoethyl methacrylate differs significantly due to a strong coordination between the monomer and copper catalyst in ATRP. Baskaran et al.²⁹ reported the ATRP of methyl vinyl ketone (MVK) using CuBr as catalyst. They failed to prepare homopolymer of MVK, because the carbonyl chromophore of MVK was participating in complexation with Cu catalyst. In the present case the coordination between $-\text{NH}_2$ group in the monomer and copper catalyst decreases the rate of ATRP. In a controlled experiment, conventional radical polymerization of Am-AdA using azobisisobutyronitrile (AIBN) led to very high conversion (89% conversion at 3 h, $M_n = 18760$, $M_w/M_n = 2.1$) during polymerization, whereas ATRP of Am-AdA shows conversion 50% in 10 h. It also indicates that the interaction of $-\text{NH}_2$ in Am-AdA with ATRP catalyst affects the polymerization reaction.

Figure 4a shows the ^1H NMR spectra of the homopolymer of Am-AdA. The resonance at $\delta = 3.74$ ppm is due to the proton of the $-\text{NH}_2$ group of the adamantyl group (designated as “a” in Figure 4a). The resonances at 1.38 and 2.28 ppm are due to the methylene ($-\text{CH}_2-$) and methine ($>\text{CH}-$) protons in the main chain backbone of the polymer (as designated as “c and d”, respectively). The resonances at 1.57 and 1.63–1.79 ppm are due to the two different types of $>\text{CH}_2$ protons in the adamantyl group (as designated as “b₁” and “b₃” respectively, Figure 4a). The resonances at 2.01 ppm is due to the $>\text{CH}-$ (designated as “b₂” in Figure 4a) proton in the adamantyl group. The small resonance at 3.65 ppm is attributed to the proton of $>\text{CH}-\text{Br}$ (chain end group of the polymer).

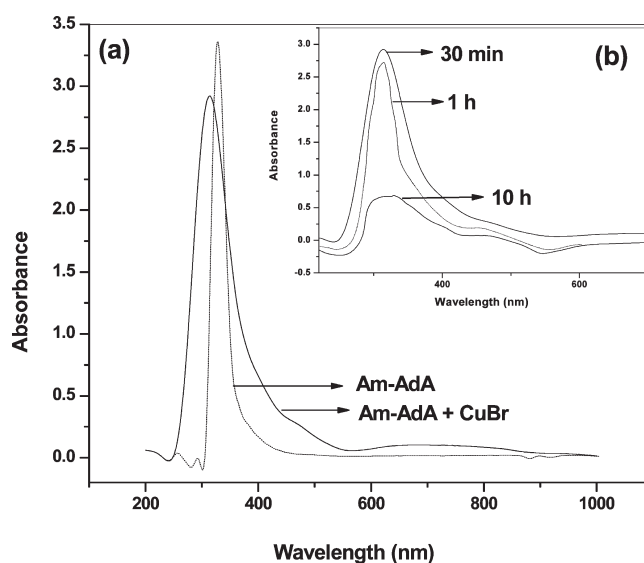


Figure 3. UV-vis spectra of (a) amino adamantyl acrylate (Am-AdA) (dotted line) and a mixture of Am-AdA and CuBr (solid line) (both at a concentration of 5.0×10^{-4} mol/L in tetrahydrofuran) and (b) UV-vis spectra of the mixture of Am-AdA and CuBr at different times.

The copolymerization of Am-AdA and MA (feed ratio 40:60) was carried out using the dNbpy/CuBr catalyst using methyl-2-bromo propionate as initiator (Scheme 2). Figure 4b shows the ^1H NMR spectrum of the PAm-AdA-co-PMA (40:60). The resonance at 3.55 ppm is attributed to the $-\text{OCH}_3$ of MA protons (designated as “e” in Figure 4b). The resonance at 3.74 ppm is due to the $-\text{NH}_2$ protons (designated as “a” in Figure 4b) of the PAm-AdA. The resonances at 1.57 [$>\text{CH}_2$ (b₁)], 1.63–1.79 [$>\text{CH}_2-$ (b₃)] and 2.01 [$>\text{CH}-$ (b₂)] ppm are due to the three types of adamantyl protons. The resonances at 1.37 and 2.29 ppm are due to the different aliphatic protons ($-\text{CH}_2-$ and $>\text{CH}-$) of the PAm-AdA and PMA protons in the main chain backbone as designated as “c and d” respectively. The copolymer composition was calculated from the integration ratio of the peak intensities of the protons $-\text{NH}_2$ ($\delta = 3.74$ ppm designated as “a” in Figure 4b) and $-\text{OCH}_3$ of ($\delta = 3.55$ ppm designated as “e” in Figure 4b) PAm-AdA and PMA units respectively. The final copolymer (PAm-AdA-co-PMA) composition was 25% of PAm-AdA and 75% of PMA. The less incorporation of PAm-AdA clearly indicates the slow reactivity or the slow rate of polymerization. In a controlled experiment, when conventional radical copolymerization of Am-AdA and MA (feed ratio 40:60) was

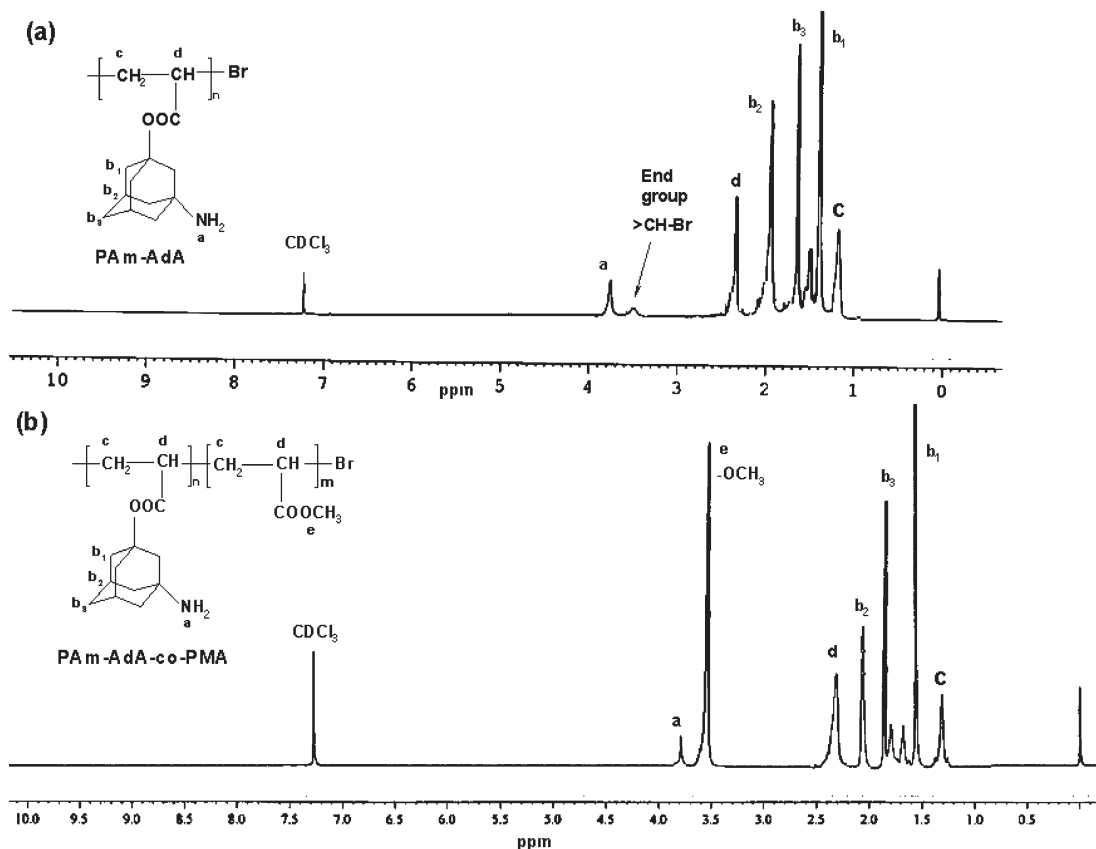


Figure 4. ^1H NMR spectra of the polymers: (a) homopolymer of poly (amino adamantyl acrylate) (PAm-AdA); (b) copolymer of poly (amino adamantyl acrylate-co-poly methyl acrylate) (PAm-AdA-co-PMA) (25:75).

carried out using AIBN as initiator, there was 76% conversion at 5 h. The final copolymer (PAm-AdA-co-PMA) composition was 56% of PAm-AdA and 44% of PMA. It clearly indicates that the complexation of copper catalyst with the monomer affects the rate of ATRP as well as its incorporation into the copolymer. It is reported that in the radical copolymerization (in conventional²² as well as in ATRP²⁴) using acrylates containing adamantyl group, the incorporation of this monomer is much higher than the other comonomer. In this case less incorporation of the PAm-AdA compared to that of PMA is attributed to complex formation between monomer (PAm-AdA) and catalyst (CuBr) which alters the reactivity of the monomers.

The presence of amino-adamantyl group in the polymers was confirmed by MALDI-TOF MS analysis (Figure 5). In the MALDI experiments, sodium trifluoroacetic acid was used as the cationic agent. All macromolecular chains have sodium ion as the cationic agent, and they were detected at m/z value 23 Da above the theoretically calculated values. The mass series (M) appearing in the MALDI-TOF-MS spectra can be expressed as follows:

$$M = M_1 + nM_r + M_{\text{end group}} + M_{\text{cation}} \quad (1)$$

Here, M_1 , M_r , $M_{\text{end group}}$, and M_{cation} are the masses of the initiator moiety (methyl-2-bromo propionate [MBrP] = 87), monomer (Am-AdA = 221), repeat unit (n), end groups ($-\text{Br}$ = 80) and cation (Na = 23), respectively, and n stands for the degree of polymerization. The isotopic distribution of each peak was compared with those peaks simulated with Isopro-3 and then the peaks were assigned carefully. Figure 5b shows the amplified MALDI spectrum of the PAm-AdA. The difference in molecular weight of each intense peak is 221 which is the molecular weight of 3-amino adamantyl acrylate (Am-AdA). The peak at 2621 is attributed to

the structure-a. It clearly shows that each macromolecular chain has methyl propionate [$-\text{CH}(\text{CH}_3)\text{CO}_2\text{CH}_3$] and $-\text{Br}$ end groups. The average molecular weight and polydispersity index (M_w/M_n) of PAm-AdA determined by MALDI was 5652 (M_n) and 1.33 (M_w/M_n) respectively ($M_{n,\text{GPC}} = 5572$ and $M_w/M_n = 1.33$). The $-\text{Br}$ end group was further confirmed by the chain extension experiment of the polymer PAm-AdA as macroinitiator and by the addition of fresh MMA. Formation of the diblock copolymer was confirmed by ^1H NMR and GPC analysis. There was shift of GPC traces toward higher MW in GPC chromatogram (Figure 6). In the ^1H NMR spectrum there was an emergence of a new peak at $\delta = 3.5$ ppm which is due to the proton of $-\text{OCH}_3$ group of PMMA part.

Reaction between Poly(amino adamantyl acrylate) (PAm-AdA) and Polyglycidyl Methacrylate (PGMA): A Supramolecular Polymer. The hydrogen bond is a unique phenomenon in structural chemistry and biology.³⁰ In supramolecular chemistry, the hydrogen bond is able to control and direct structures of molecular assemblies, because it is sufficiently strong and sufficiently directional.³¹ The polyacrylates bearing amantadine polymers can have interesting applications because of the presence of the hydrogen-bonding motifs ($-\text{NH}_2$) for the design of supramolecular architectures. The presence of $-\text{NH}_2$ group in the polymers prepared so far was further confirmed by the thermal cross-linking reaction between amine and epoxy group. This kind of reaction is used in many applications such as in adhesives, in protective coatings, in microelectronics, and in different composite applications.^{32–35} The epoxy-amine is also used to prepare porous thermosetting materials which can be used as selective permeation membranes³² and as substrates for nanocomposite fabrication.³³ In this investigation we carried out the reaction between poly (amino adamantyl acrylate)

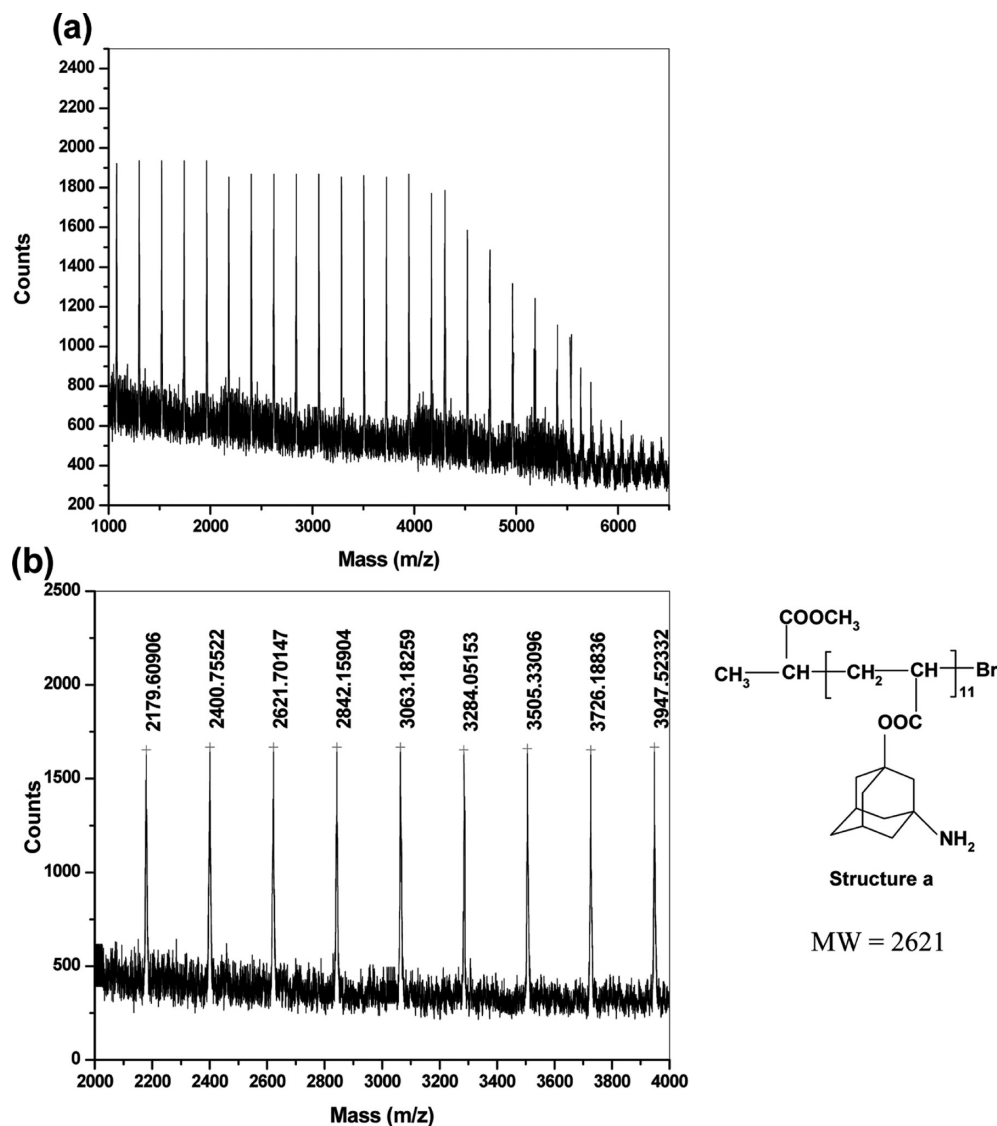


Figure 5. Matrix assisted laser desorption/ionization time-of-flight mass spectrum of poly(amino adamantyl acrylate): (a) whole mass spectrum; (b) Amplified region.

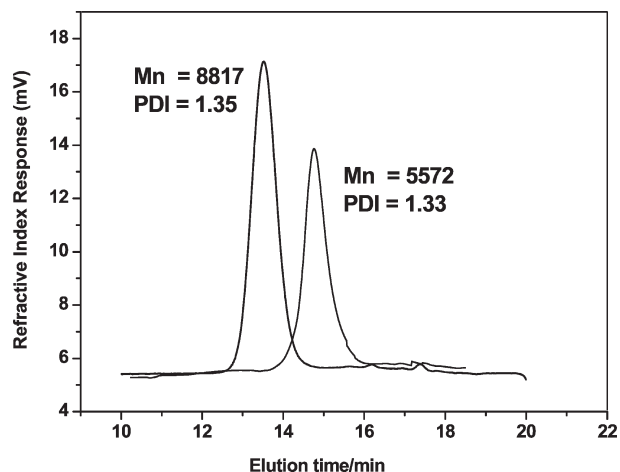


Figure 6. Gel permeation chromatography traces of poly(amino adamantyl acrylate) macroinitiator and poly(methyl methacrylate-*b*-amino adamantyl acrylate) prepared by chain extension reaction.

[prepared by ATRP, $M_n = 5572$ and $M_w/M_n = 1.33$] and poly(glycidyl methacrylate) [prepared by ATRP, $M_n = 5865$

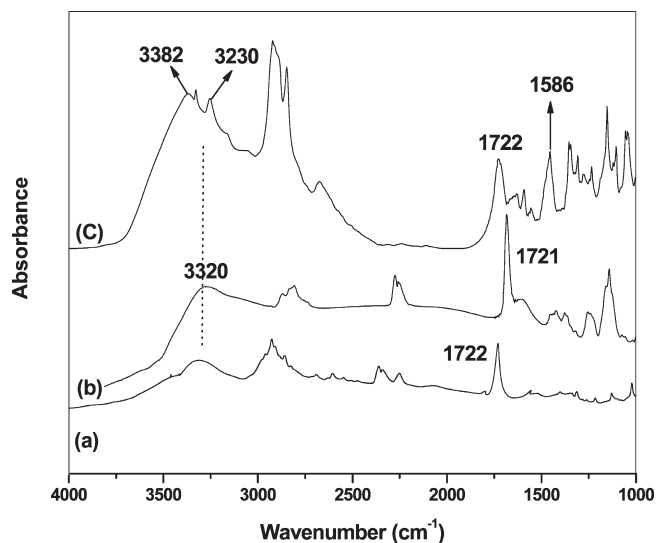


Figure 7. FTIR spectra for (a) Poly(glycidyl methacrylate) (PGMA), (b) Poly(amino adamantyl acrylate) (PAm-AdA), and (c) PGMA-PAm-AdA (1:1) (polymer VI).

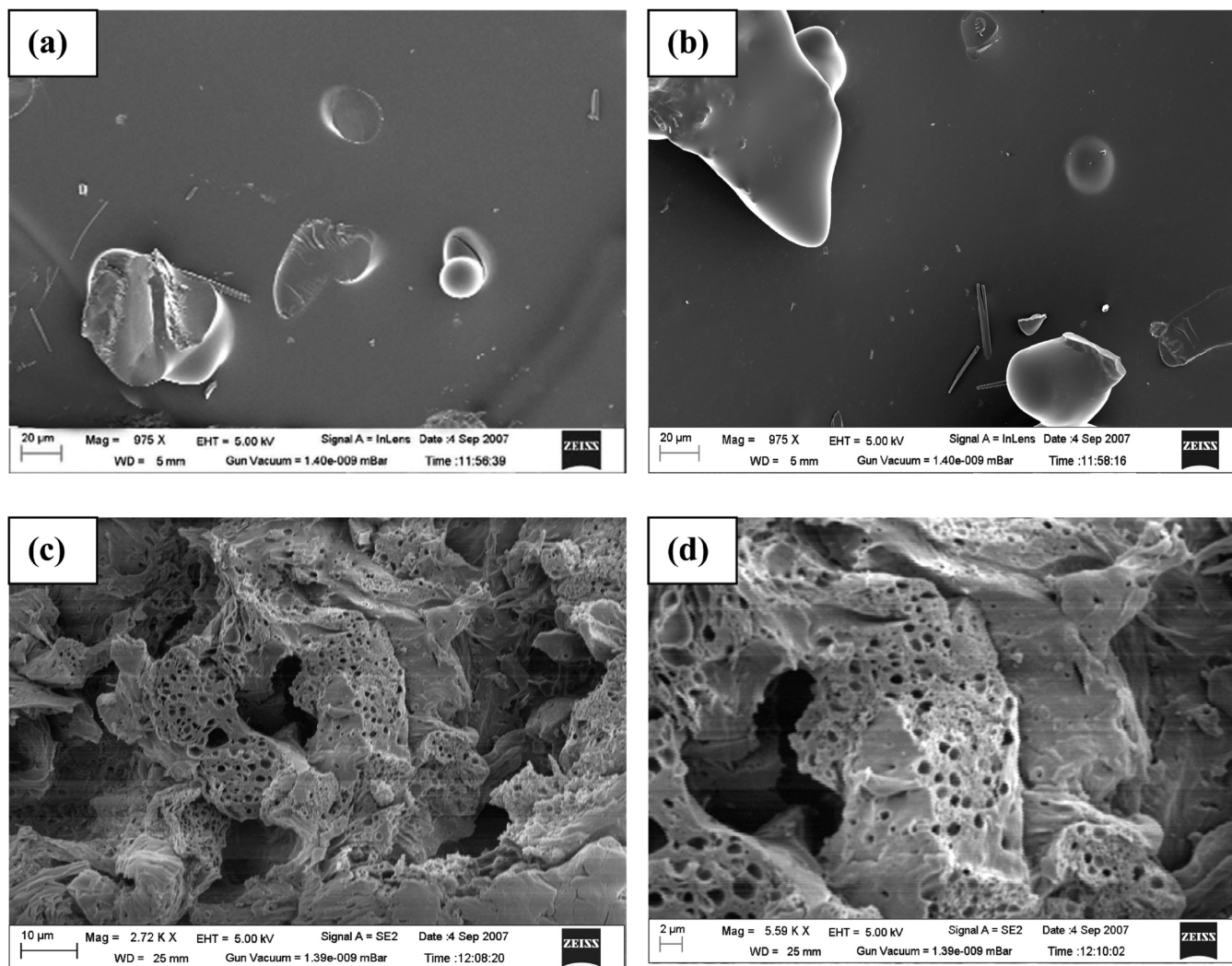


Figure 8. Field-emission scanning electron micrographs of the samples: (a) poly(glycidyl methacrylate) (PGMA), (b) poly(amino adamantyl acrylate) (PAm-AdA), and (c and d) polymer VI [PGMA-PAm-AdA] in low and high magnifications, respectively.

and $M_w/M_n = 1.21$] having epoxy pendant group. Scheme 3 shows the reaction between the amine group and the epoxy group in the tailor-made polymers which leads to the formation of $-NH-$ and $-OH$ groups and subsequently the intermolecular hydrogen bonding.

The reaction between amine and epoxy group was investigated by FTIR spectroscopy as shown in Figure 7. PGMA (Figure 7a) shows the epoxy band at 910 cm^{-1} and the carbonyl band at 1722 cm^{-1} . PAm-AdA (Figure 7b) shows broad bands at 3320 cm^{-1} due to the primary amine ($-NH_2$) and the peak at 1721 cm^{-1} due to the carbonyl group (CO). Figure 7c shows the reaction between PAm-AdA and PGMA. In this case a new strong band appears at 3382 cm^{-1} due to the formation of hydroxyl groups ($-OH$) by the ring-opening of the epoxy group in the PGMA unit. Normally the free OH band appears at around 3600 cm^{-1} .³⁶ The broad absorption band positions at $3376\text{--}3387\text{ cm}^{-1}$ are attributed to the hydrogen-bonded $-OH$. It indicates that the hydroxyl groups of PGMA-PAm-AdA (polymer VI) are mostly hydrogen bonded. Interestingly, there was emergence of a new shoulder peak at 3230 cm^{-1} which is attributed to the formation of the secondary amine ($-NH-$). These FTIR spectra show clear evidence for the reaction of PGMA with PAm-AdA and the formation of hydrogen bonding in the polymer.

Figure 8 shows the surface topography of the hydrogen-bonded polymer (VI) by field emission scanning electron

microscopy (FESEM) analysis. Figure 8a and 8b show the FESEM images of PGMA and PAm-AdMA respectively, and figure 8c and 8d show the FESEM images of the hydrogen-bonded polymer (polymer VI) at different magnifications. It is observed that the hydrogen-bonded polymer (polymer VI) has the porous network structure (Figure 8, parts c and d). Raman et al.³⁷ reported the formation of nanoporous polymer materials during the reaction between diglycidyl ether of bisphenol A and 4,4'-methylenebis(cyclohexylamine) and proved this by SEM analysis. During the step-growth polymerization reaction of epoxy-amine system, OH group in the polymer interacts with the oxygen in THF to form hydrogen bonding, resulted in the final polymer structure with porous network.^{37,38} In our case the porous network structure is due to the reaction between epoxy group (in the tailor-made PGMA) and $-NH_2$ group (in PAm-AdA) and due to the hydrogen bonding between the $-OH$ group and $-NH-$ generated *in situ* thereof (Scheme 3). The pore size was calculated to be $0.62\text{ }\mu\text{m}$ using the image processing software Image tool version 3.0.

The evidence of hydrogen bonding interaction of polymer VI was confirmed by molecular modeling using DMol³ software. The optimization of the hydrogen-bonded structure was made by using the Gaussian 03 package.³⁹ The initial structure (the output hydrogen-bonded structure from DMol³) as an input file was made through Gauss View.³⁹

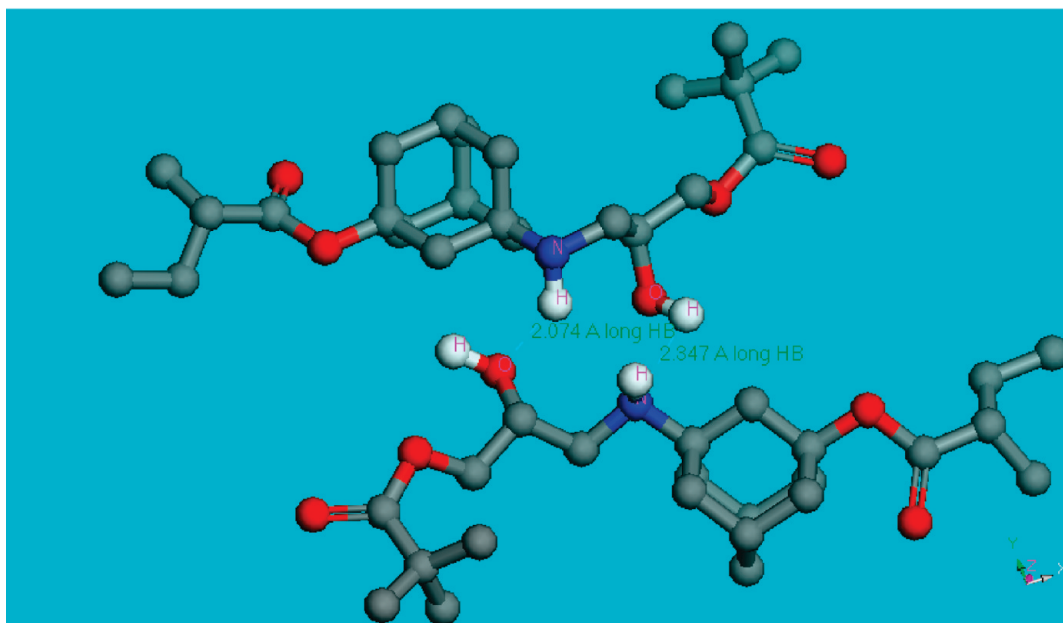
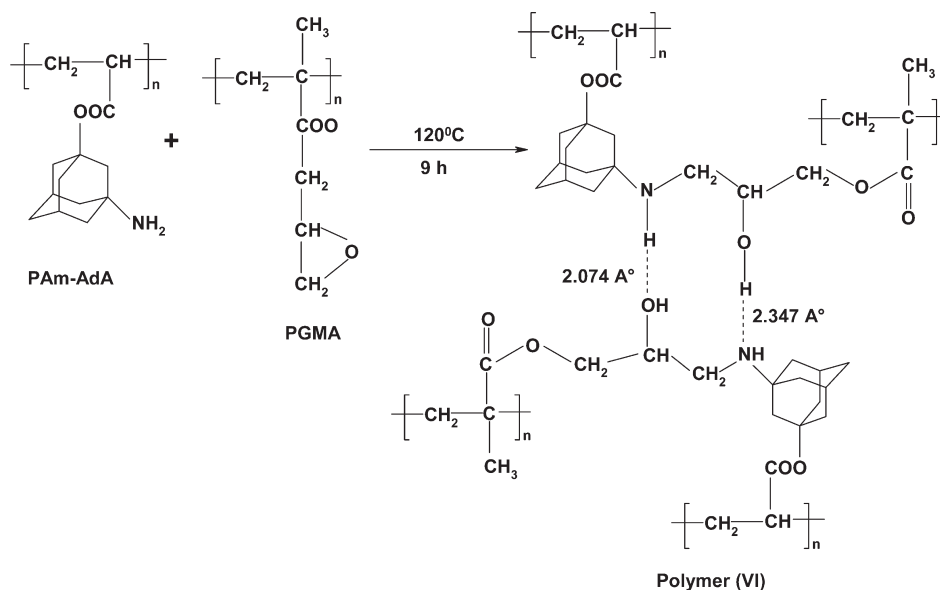


Figure 9. Optimized 3D structure of the hydrogen-bonded polymer **VI** (as shown in Scheme 3).

Scheme 3. Reaction between Poly(amino adamantyl acrylate) (PAm-AdA) and Poly(glycidyl methacrylate) (PGMA) and Formation of Hydrogen Bonding in the Polymer Network



The results of the Gaussian output of the hydrogen bonding atoms were visualized with the help of Gauss View³⁹ and the assignment of the structure were made. The hydrogen bond lengths of —OH and —NH— are found to be 2.074 and 2.347 Å, respectively. The optimized structure of polymer **VI** is shown in Figure 9. This study clearly confirmed the formation of hydrogen bond in the polymer.

DSC Analysis. DSC analysis showed the T_g of PAm-AdA and PGMA at 131 and 55 °C, respectively (Figure 10). The higher T_g of PAm-AdA is due to the presence of bulky and rigid adamantyl group which restricts the chain mobility. The post polymerization reaction between the two tailor-made polymers PAm-AdA and PGMA leads to new polymer system (polymer **VI**) with complex architecture (like reaction between —NH_2 and oxirane ring as well as H-bonding). This new polymeric material (polymer **VI**) prepared by the reaction between PAm-AdA and PGMA (1:1) showed a T_g of

63 °C (Figure 10). This low T_g , much lower than expected in the case of this cross-linked structure, may be due to the formation of a flexible side chain (—O— linkage) (Figure 10) due to the opening of epoxy group.⁴⁰ It is reported that the oxirane ring-opening of PGMA forms flexible chain⁴⁰ by elongation of the side chain (—O— linkage), and thus it reduces the T_g of the material. Interestingly, the DSC thermogram shows an endotherm at 103 °C, which may be attributed to the breakage of H-bonds⁴¹ that cause softening to the polymer chains.

Conclusion

Well-defined tailor-made homo as well as copolymer of amino adamantyl acrylate was successfully prepared by atom transfer radical polymerization. The presence of amino adamantyl (amantadine) group reduces the rate of ATRP, because of the interaction of amine group of amantadine with copper catalyst. This was

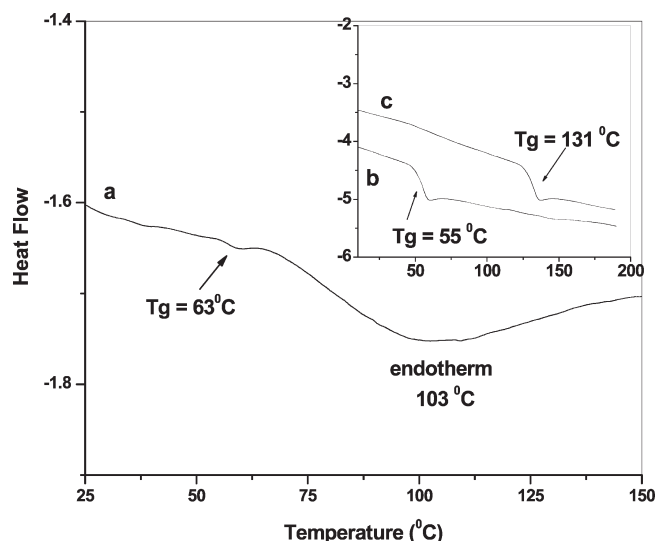


Figure 10. Differential scanning calorimetric thermograms of (a) polymer VI (as shown in Scheme 3), (b) poly(glycidyl methacrylate), and (c) poly(amino adamantyl acrylate).

confirmed by UV-vis spectroscopy studies and the controlled experiments of AdMA or MA with CuBr. The end group of the polymer was confirmed by ^1H NMR spectroscopy, matrix assisted laser desorption ionization time-of-flight mass spectrometry and chain extension experiment. This analysis showed that the polymers had well-defined molecular weight and amino adamantyl functional group as well as all polymer chain had a well-defined end group. Interestingly, the tailor-made PAM-AdA reacted with tailor-made PGMA to prepare porous network structure having H-bonding. It was confirmed FT-IR, field emission scanning electron microscopy as well as by 3D-modeling studies. Differential scanning calorimetry analysis of the cross-linked porous polymer showed an endotherm at 103 °C indicating the presence of H-bonding in the polymer. These porous hydrogen-bonded materials may have potential applications in drug encapsulation and drug delivery in biomedical applications.

Acknowledgment. The authors gratefully acknowledge Department of Science & Technology (DST), New Delhi, India, and IIT, Kharagpur, India (for the sanction of ISIRD project), for the financial support.

References and Notes

- (1) (a) Bednarek, M.; Biedron, T.; Kubisa, P. *Macromol. Rapid Commun.* **1999**, *20*, 59–65. (b) Matyjaszewski, K.; Wang, J. S. *Macromolecules* **1995**, *28*, 7901–7010.
- (2) Shipp, D. A.; Wang, J. L.; Matyjaszewski, K. *Macromolecules* **1998**, *31*, 8005–8008.
- (3) Grimaud, T.; Matyjaszewski, K. *Macromolecules* **1997**, *30*, 2216–2218.
- (4) Kato, M.; Kamigaito, M.; Sawamoto, M.; Higashimura, T. *Macromolecules* **1995**, *28*, 1721–1723.
- (5) Ando, T.; Kamigaito, M.; Sawamoto, M. *Macromolecules* **1998**, *31*, 6708–6711.
- (6) Zhang, X.; Matyjaszewski, K. *Macromolecules* **1999**, *32*, 7349–7353.
- (7) (a) Sadhu, V. B.; Pionteck, J.; Voigt, D.; Komber, H.; Fischer, D.; Voit, B. *Macromol. Chem. Phys.* **2004**, *205*, 2356–2365. (b) Brzezinska, K. R.; Deming, T. J. *Macromol. Biosci.* **2004**, *4*, 566–569.
- (8) Beyou, E.; Jarroux, N.; Zydowicz, N.; Chaumont, P. *Macromol. Chem. Phys.* **2001**, *202*, 974–979.
- (9) Greenberg, A.; Breneman, C. M.; Liebman, J. F. *The Amide Linkage: Selected Structural Aspects in Chemistry, Biochemistry, and Materials Science*; Wiley: New York, 2000.

- (10) Jasys, J. V.; Lombardo, F.; Appleton, T. A.; Bordner, J.; Ziliox, M.; Volkmann, R. A. *J. Am. Chem. Soc.* **2000**, *122*, 466–473.
- (11) Elliot, J. *J. Am. Med. Assoc.* **1979**, *242*, 2383.
- (12) Kelly, J. M.; Quack, G.; Miles, M. M. *Antimicrobiol. Agents Chemother.* **2001**, *45*, 1360–1366.
- (13) Hagan, J. J.; Middlemiss, D. N.; Sharpe, P. C.; Poste, G. H. *Trends Pharmacol. Sci.* **1997**, *18*, 156–163.
- (14) Davies, W. L.; Grunert, R. R.; Haff, R. F.; McGahen, J. W.; Neumayer, E. M.; Paulshock, M.; Watts, J. C.; Wood, T. R.; Hermann, E. C.; Hoffmann, C. E. *Science* **1964**, *144*, 862–863.
- (15) Hoffmann, C. E. Amantadine HCl and Related Compounds. In *Selective Inhibitors of Viral Functions*; Carter, W. A., Ed.; CRC Press: Cleveland, OH, 1973; pp 199–211.
- (16) Grunert, R. R.; McGahen, J. W.; Davies, W. L. *Virology* **1965**, *26*, 262–269.
- (17) Dolin, R.; Reichman, R. C.; Madore, H. P.; Maynard, R.; Lindon, P. M.; Jones, J. A. W. *N. Engl. J. Med.* **1982**, *307*, 580–584.
- (18) Couch, R. B.; Jackson, G. G. *J. Infect. Dis.* **1976**, *134*, 516–527.
- (19) Bryson, Y. J.; Monahan, C.; Pollack, M.; Shields, W. D. A. *J. Infect. Dis.* **1980**, *141*, 543–547.
- (20) (a) Gao, Y.; Katsuraya, K.; Kaneko, Y.; Mimura, T.; Nakashima, H.; Uryu, T. *Macromolecules* **1999**, *32*, 8319–8324. (b) Dhal, P. K.; Farley, S. R. H.; Mandeville, W. H.; Neenan, T. X. *Polymer Drugs in Encyclopedia of Polymer Science and Technology*, 3rd Ed.; Wiley, New York, 2002; pp 555–580.
- (21) Yoshida, T.; Akasaka, T.; Choi, Y.; Hattori, K.; Yu, B.; Mimura, T.; Kaneko, Y.; Nakashima, H.; Aragaki, E.; Premanathan, M.; Yamamoto, N.; Uryu, T. *J. Polym. Sci., Part A: Polym. Chem.* **1999**, *37*, 789–800.
- (22) Matsumoto, A.; Tanaka, S.; Otsu, T. *Macromolecules* **1991**, *24*, 4017–4024.
- (23) (a) Burns, W.; Grant, D.; McKerver, M. A.; Step, G. *J. Chem. Soc., Perkin Trans.* **1976**, *1*, 234–238. (b) Ishizone, T.; Tajima, H.; Torimae, H.; Nakahama, S. *Macromol. Chem. Phys.* **2002**, *203*, 2375–2384. (c) Acar, H. Y.; Jensen, J. J.; Thigpen, K.; McGowen, J. A.; Mathias, L. J. *Macromolecules* **2000**, *33*, 3855–3859.
- (24) Kavitha, A. A.; Singha, N. K. *J. Polym. Sci., Part A: Polym. Chem.* **2008**, *46*, 7101–7113.
- (25) (a) Weiss, J. F.; Tollin, G.; Yoke, J. T. III. *Inorg. Chem.* **1964**, *3*, 1344–1348. (b) Simon, A.; Hamann, H.; Arnold, F. *Rev. Chim. Acad. Rep. Populaire, Roumaine* **1962**, *7*, 531.
- (26) Dong, H.; Matyjaszewski, K. *Macromolecules* **2008**, *41*, 6868–6870.
- (27) (a) Braunecker, W. A.; Pintauer, T.; Tsarevsky, N. V.; Kickelbick, G.; Matyjaszewski, K. *J. Organomet. Chem.* **2005**, *690*, 916–924.
- (28) Lad, J.; Harrison, S.; Mantovani, G.; Haddleton, D. M. *Dalton Trans.* **2003**, 4175–4180.
- (29) Mittal, A.; Sivaram, S.; Baskaran, D. *Macromolecules* **2006**, *39*, 5555–5558.
- (30) Desiraju, G. R.; Steiner, T. *The Weak Hydrogen Bond in Structural Chemistry and Biology*; Oxford university press: New York 2001, p 1.
- (31) Hoogenboom, R.; Schubert, U. S. *Chem. Soc. Rev.* **2006**, *35*, 622–629.
- (32) (a) Fang, J.; Kita, H.; Okamoto, K. *J. Membr. Sci.* **2001**, *182*, 245–256. (b) Wang, Y.; Hirakawa, S.; Wang, H.; Tanaka, K.; Kita, H.; Okamoto, K. *J. Membr. Sci.* **2002**, *199*, 13–27.
- (33) Raman, V. I.; Palmese, G. R. *Colloids Surf. A* **2004**, *241*, 119–125.
- (34) (a) Raman, V. I.; Palmese, G. R. *Macromolecules* **2005**, *38*, 6923–6930. (b) Buist, G. J.; Barton, J. M.; Howlin, B. J.; Jones, J. R.; Parker, M. J. *J. Mater. Chem.* **1996**, *6*, 911–915. (c) Sauvart, V.; Halary, J. L. *Compos. Sci. Technol.* **2002**, *62*, 481–486.
- (35) (a) Lee, K. J.; Kim, Y. W.; Koh, J. H.; Kim, J. H. *J. Polym. Sci., Part B: Polym. Phys.* **2007**, *45*, 3181–3188. (b) Yang, J.; Huang, K.; Pu, Z.; Gong, Y.; Li, H.; Hu, C. *J. Mole. Struct.* **2006**, *789*, 162–168.
- (36) Noto, D. V.; Longo, D.; Munchow, V. *J. Phys. Chem. B* **1999**, *103*, 2636–2646.
- (37) Raman, V. I.; Palmese, G. R. *Langmuir* **2005**, *21*, 1539–1546.
- (38) Mijovic, J.; Fishbain, A.; Wijayat, J. *Macromolecules* **1992**, *25*, 979–985.
- (39) Singh, D.; Srivastava, S. K.; Ojha, A. J.; Asthana, B. P.; Singh, R. K. *J. Mol. Struct. Theochem* **2007**, *819*, 88–94.
- (40) Mark, H. F. In *Encyclopedia of Polymer Science and Technology*; Mark, H. F., Ed.; John Wiley & Sons: New York, 2004; Vol. 9, p 768.
- (41) (a) Folmer, B. J. B.; Sijbesma, R. P.; Versteegen, R. M.; Rijt, J. A. J. v.; Meijer, E. W. *Adv. Mater.* **2000**, *12*, 874–878. (b) Scherman, O. A.; Ligthart, G. B. W. L.; Ohkawa, H.; Sijbesma, R. P.; Meijer, E. W. *Proc. Natl. Acad. Sci. U.S.A.* **2006**, *103*, 11850–11855.